

Binarized Coherent Optical Receiver Based on Opto-Electronic Neural Network

Zhenming Yu , Xu Zhao, Sigang Yang , Hongwei Chen , and Minghua Chen 

Abstract—The resolution of analog to digital converter (ADC) and the power consumption of digital signal processing (DSP) are becoming the bottleneck of optical communication system. To acquire and recover signals with low resolution ADCs, we propose a binarized coherent optical receiver based on opto-electronic neural network, which consists of three layers, the broadcast layer, the optical neural layer, and the electronic neural layer. The broadcast layer that composed of Mach-Zehnder interferometers (MZIs) is to duplicate and select the input optical signal into the opto-electronic neural network. The optical neural layer is constituted by specially designed structures to map the binarized weights into optical domain, which can be integrated on silicon together with the broadcast layer. The one-bit vertical resolution ADCs act as the binarized activation after the optical neural layer. This binarized coherent optical receiver is demonstrated in simulation of 50-Gb/s single polarization (SP) QPSK system and 100-Gb/s polarization multiplexing (PDM) QPSK system. The one-bit vertical resolution ADCs can be utilized to recover the complex modulation format signal successfully. The broadcast layer and the optical neural layer can be integrated based on silicon, which could increase the calculation speed and reduce the energy consumption of the total system.

Index Terms—Optical neural network, analog to digital converter, binarized coherent optical receiver.

I. INTRODUCTION

THE explosive growth of information continuously promotes the capacity of optical fiber communication systems. Wavelength-division multiplexing (WDM) is an effective way to improve the capacity of optical communication systems [1]–[6].

Manuscript received January 9, 2019; revised June 16, 2019; accepted July 22, 2019. Date of publication July 25, 2019; date of current version August 16, 2019. This work was supported in part by the National Key R&D Program of China under Grants 2018YFB2201802 and 2018YFB2201803, in part by NSFC Program under Grants 61771285, 61431003, and 61625104, in part by the Beijing Municipal Science and Technology Commission under Grant Z181100008918011, and in part by the Fundamental Research Funds for the Central Universities. (Corresponding author: Zhenming Yu.)

Z. Yu was with the Department of Electrical Engineering and the Beijing National Research Center for Information Science and Technology, Tsinghua University, Beijing 100084, China. He is now with the State Key Laboratory of Information Photonics and Optical Communications, Beijing University of Posts and Telecommunications, Beijing 100876, China (e-mail: yuzhenming@bupt.edu.cn).

X. Zhao, S. Yang, H. Chen, and M. Chen are with the Department of Electrical Engineering and the Beijing National Research Center for Information Science and Technology, Tsinghua University, Beijing 100084, China (e-mail: 1361848000@qq.com; ysg@tsinghua.edu.cn; chenhw@tsinghua.edu.cn; chenmh@tsinghua.edu.cn).

Color versions of one or more of the figures in this article are available online at <http://ieeexplore.ieee.org>.

Digital Object Identifier 10.1109/JSTQE.2019.2931251

However, to further improve the capacity with more channels, more wavelength are utilized, meaning closer channel space and consequently more system complexity. Meanwhile, advanced modulation formats together with coherent optical receiver are exploited to increase the spectral efficiency [7]–[15]. This combination could lower the network cost per bit with the increasing of transported bits, making it dominant in optical communication systems [16]–[21]. Nonetheless, this approach depends on high-performance analog to digital converters (ADCs) and complex digital signal processing (DSP). On the one hand, complex order modulation formats demand higher resolution of ADC [22]–[25]. It is inevitable that the price of ADC grows exponentially as the resolution increases. On the other hand, more complicated DSP in electronic domain results in much more power consumption. Currently, the cost of ADC and the complexity of DSP in the receiver are becoming the bottleneck of optical communication systems. Therefore, solely relying on the performance of ADCs and DSP may not be the best way for optical communication in the future.

Optical signal processing has not only the advantages of high speed, large capacity but also the merits of low energy consumption and low latency [26]–[30]. Moreover, with the emergence and rapid development of large-scale silicon-based photonic integrated microsystem, the cost and energy consumption of the devices are further reduced significantly [31]–[35]. Therefore, as the approaching of electronic limits, optical signal processing will play an important role in increasing processing speed and decreasing energy consumption. Recently, optical neural network based on silicon photonics or passive diffractive layers are proposed to improve the computational speed and power efficiency [36]–[39]. However, it is hard to realize complex logic calculation and deep learning for optical neural network at present. In contrast, electronic neural network has been extensively researched and applied in multiple fields, such as speech recognition, computer vision, medical care and intelligent game [40]–[44]. Electronic neural network is finer, more flexible, easier to operate and more suitable for deep learning. Nonetheless, it also has some drawbacks such as high energy consumption and low processing speed. Therefore, it is an exciting initiative to combine the advantages of optical and electronic neural network.

In this paper, we propose a binarized coherent optical receiver based on opto-electronic neural network, which is applicable to complex modulation formats by using the low vertical resolution ADCs of only one-bit. In order to achieve the demodulation of complex modulation formats with the one-bit vertical resolution

ADCs, we utilize the binarized neural network to process the received signals. Binarized neural network is proposed by Matthieu Courbariaux *et al*, which could employ binarized weights and activations at run-time without suffering any loss in classification accuracy [45]. Therefore, the one-bit vertical resolution ADC can be regarded as the activations of the binarized neural network. Then we propose the structure of binarized coherent optical receiver based on binarized neural network for signal detection in coherent optical system. There are three parts, *i.e.*, the broadcast layer, the optical neural layer, and the electronic neural layer in the binarized coherent optical receiver. We train an artificial neural network (ANN) with binarized weights and activations in the first layer to recover the signal after conventional coherent detection. And we design two special structures to map the binarized weights in the optical domain for SP and PDM system respectively. In the binarized coherent optical receiver, the received optical signal is firstly sent to the broadcast layer that composed of MZIs to duplicate and select the input optical signal to the opto-electronic neural network. Then the specially designed structures are utilized to map the first layer of the trained ANN before. The broadcast neural layer and optical neural layer can be integrated based on silicon, which could increase the calculation speed and reduce the energy consumption of the total system. The one-bit vertical resolution ADCs are used as the binarized activations of the first layer. The binarized digital signal that sampled by ADCs is then processed by the electronic neural layer with conventional weights and activations, which are same with the trained ANN before. We conduct simulation of 50-Gb/s SP-QPSK system and 100-Gb/s PDM-QPSK system to demonstrate the binarized coherent optical receiver. The simulation results show that this binarized coherent optical receiver could work well to recover the signal of complex modulation format.

II. BINARIZED NEURAL NETWORK

Binarized neural networks are the neural networks with binarized weights and activations at run-time, which could drastically reduce memory size and accesses, and replace most arithmetic operations with bit-wise operations [42]. Fig. 1 shows the structure of the binarized neural network. Only using the weights and the activations to either +1 or -1, binarized neural networks could substantially improve power-efficiency without suffering any loss in classification accuracy [45].

In order to achieve binarization, the deterministic binarization function is applied:

$$x^b = \text{Sign}(x) = \begin{cases} +1 & \text{if } x \geq 0 \\ -1 & \text{otherwise} \end{cases} \quad (1)$$

where x^b is the binarized variable, x is the real-valued variable. This method is easy to implement and shows better performance in practice. The most important in binarized neural networks is the training of the weights. The weight parameters of the binarized networks must be real valued in the training, and then the real-valued weights are binarized to obtain the binarized value weight parameters. However, the backpropagation of binarized neural networks is difficult to realize because the derivative of the

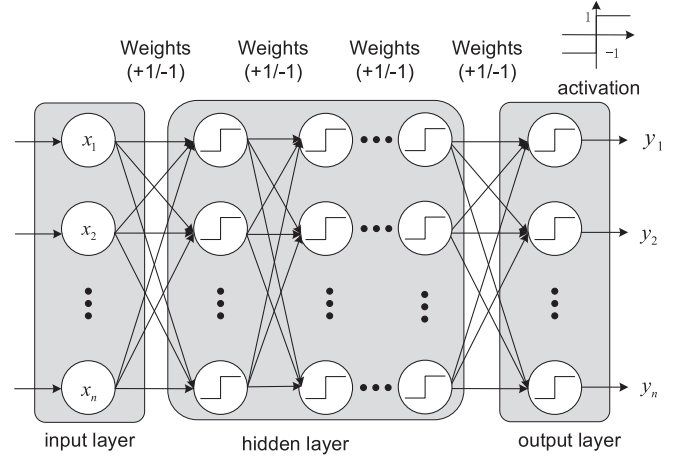


Fig. 1. Structure of binarized neural network.

Sign function is zero almost everywhere. Therefore, an approach of straight-through estimator is applied, which means using *Hard Tanh* function instead of *Sign* function in the calculating of gradient, as shown in:

$$H \tanh(x) = \text{Clip}(x, -1, 1) = \max(-1, \min(1, x)) \quad (2)$$

This approach can both preserve the information of gradient and maintain the performance. Note that the obtaining of the gradient is the gradient of the binarized weights rather than the real-type weights before binarization, because the weights before binarization do not really participate in the forward propagation of the network [45].

III. OPTO-ELECTRONIC NEURAL NETWORK

In typical coherent optical communication system, the transmitted I/Q RF signals are moved to the optical carrier by the optical I/Q modulator, which means both the amplitude and phase of the optical carrier are utilized to carrier the information. In the receiver, a phase-diversity homodyne receiver is applied to obtain the *I* and *Q* of the complex signal. Then the analog *I* and *Q* signals are converted to digital signals using the ADCs with high vertical resolution. Afterwards, the received digital signals are processed with DSP to recover the transmitted signals.

ANN can be applied for signal recovery in the receiver which has been demonstrated in [46]–[49]. In order to use the ADC of one bit vertical resolution instead of high vertical resolution, we utilize the binarized neural network in the optical domain and common neural network in the electronic domain, which implies a combination of optical and electronic neural networks, as shown in Fig. 2. In this opto-electronic neural network, the first layer is the binarized neural network with binarized weights and activations. The ADCs of one bit vertical resolution can be regarded as the binarized activation. The following layers are conventional ANN in the electronic domain. Therefore, the remaining problem is the realization of the binarized weights in the optical domain. Here we propose two structures of the

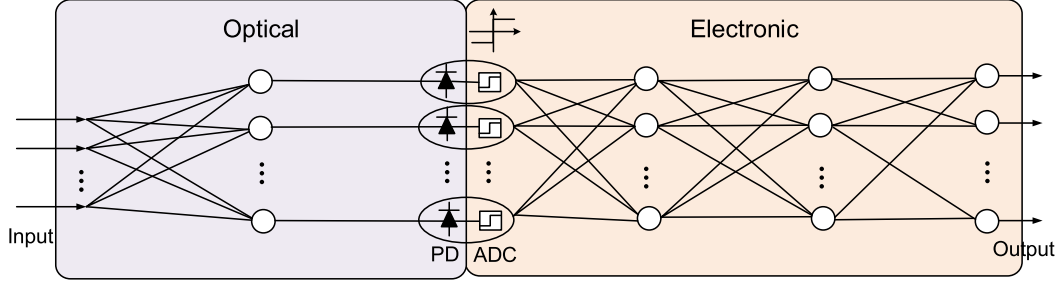


Fig. 2. Opto-electronic neural network architecture. PD: photodiode; ADC: Analog to digital converter.

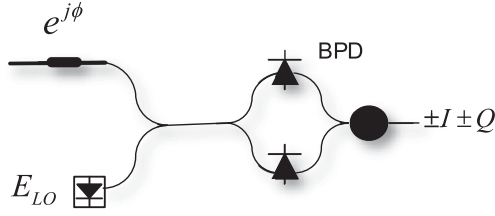


Fig. 3. Structure of optical binarized weights for single polarization system. BPD: balanced photodiode.

optical binarized weights for SP system and PDM system, respectively.

A. Optical Binarized Weights in Single Polarization System

In the single polarization coherent optical communication system, we utilize a phase shifter, an optical mixer and an balanced photodiode (BPD) to map the optical binarized weights, as shown in Fig. 3. The received optical signal E_s can be written as:

$$E_s(t) = A_s(t) \exp(j\omega_s t) \quad (3)$$

where $A_s(t)$ is the complex amplitude expressed as $I + jQ$, and ω_s is the angular frequency. Similarly, the LO is written as:

$$E_{LO}(t) = A_{LO}(t) \exp(j\omega_{LO} t) \quad (4)$$

where A_{LO} is the constant complex amplitude and ω_{LO} is the angular frequency of LO. If the phase shifter is set zero, the real part of the complex signal, *i.e.*, I , will be obtained in the receiver after the mixing of E_s and E_{LO} and the balanced PD, just as the conventional coherent optical receiver. If the optical signal E_s is introduced a phase shift by the phase shifter, the real part of the complex signal will be the aliasing of real part I and imaginary part Q , then the received signal after the optical mixer and balanced PD also be changed correspondingly, which is expressed as:

$$I \cos \phi + Q \sin \phi \quad (5)$$

Especially, if the angle of the phase shifter is set as $\pi/4$, $3\pi/4$, $5\pi/4$, or $7\pi/4$, the received signal will be $I + Q$, $I - Q$, $-I - Q$, or $-I + Q$, which implies that the binarized optical weights are applied to the real part I and imaginary part Q , as shown in Table I.

TABLE I
MAPPING OF PHASE SHIFTERS TO WEIGHTS FOR SINGLE POLARIZATION SYSTEM

ϕ	Output	Weights
$\pi/4$	$I+Q$	(1,1)
$3\pi/4$	$I-Q$	(1,-1)
$5\pi/4$	$-I-Q$	(-1,-1)
$7\pi/4$	$-I+Q$	(-1,1)

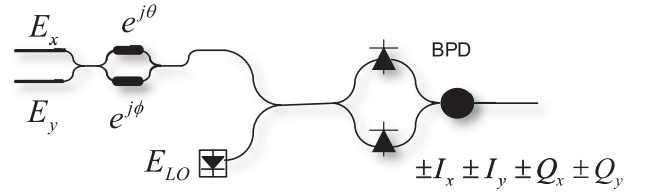


Fig. 4. Structure of optical binarized weights for polarization multiplexing system. BPD: balanced photodiode.

B. Optical Binarized Weights in Polarization Multiplexing System

In the polarization multiplexing coherent optical communication system, we utilize two phase shifters, a 3 dB fiber coupler, an 180° optical mixer and an balanced PD to realize the optical binarized weights, as shown in Fig. 4. The two orthogonal polarization signals E_x and E_y can be written as:

$$E_x(t) = A_x(t) \exp(j\omega_s t) \quad (6)$$

$$E_y(t) = A_y(t) \exp(j\omega_s t) \quad (7)$$

where $A_x(t)$ is the complex amplitude expressed as $I_x + jQ_x$, $A_y(t)$ is the complex amplitude expressed as $I_y + jQ_y$, and ω_s is the angular frequency. The output after the phase shifters and optical coupler can be expressed as:

$$\begin{aligned} \begin{bmatrix} E'_x \\ E'_y \end{bmatrix} &= \begin{bmatrix} 1/\sqrt{2} & j/\sqrt{2} \\ j/\sqrt{2} & 1/\sqrt{2} \end{bmatrix} \begin{bmatrix} E_x \cdot e^{j\theta} \\ E_y \cdot e^{j\phi} \end{bmatrix} \\ &= \begin{bmatrix} E_x \cdot e^{j\theta}/\sqrt{2} + E_y \cdot e^{j(\phi+\pi/2)}/\sqrt{2} \\ E_x \cdot e^{j(\phi+\pi/2)}/\sqrt{2} + E_y \cdot e^{j\theta}/\sqrt{2} \end{bmatrix} \end{aligned} \quad (8)$$

TABLE II
MAPPING OF PHASE SHIFTERS TO WEIGHTS FOR POLARIZATION
MULTIPLEXING SYSTEM

θ	ϕ	Output	Weights
$7\pi/4$	$5\pi/4$	$I_x + Q_x + I_y + Q_y$	(1,1,1,1)
$5\pi/4$	$5\pi/4$	$-I_x + Q_x + I_y + Q_y$	(-1,1,1,1)
$\pi/4$	$5\pi/4$	$I_x - Q_x + I_y + Q_y$	(1,-1,1,1)
$3\pi/4$	$5\pi/4$	$-I_x - Q_x + I_y + Q_y$	(-1,-1,1,1)
$7\pi/4$	$7\pi/4$	$I_x + Q_x - I_y + Q_y$	(1,1,-1,1)
$5\pi/4$	$7\pi/4$	$-I_x + Q_x - I_y + Q_y$	(-1,1,-1,1)
$\pi/4$	$7\pi/4$	$I_x - Q_x - I_y + Q_y$	(1,-1,-1,1)
$3\pi/4$	$7\pi/4$	$-I_x - Q_x - I_y + Q_y$	(-1,-1,-1,1)
$7\pi/4$	$3\pi/4$	$I_x + Q_x + I_y - Q_y$	(1,1,1,-1)
$5\pi/4$	$3\pi/4$	$-I_x + Q_x + I_y - Q_y$	(-1,1,1,-1)
$\pi/4$	$3\pi/4$	$I_x - Q_x + I_y - Q_y$	(1,-1,1,-1)
$3\pi/4$	$3\pi/4$	$-I_x - Q_x + I_y - Q_y$	(-1,-1,1,-1)
$7\pi/4$	$\pi/4$	$I_x + Q_x - I_y - Q_y$	(1,1,-1,-1)
$5\pi/4$	$\pi/4$	$-I_x + Q_x - I_y - Q_y$	(-1,1,-1,-1)
$\pi/4$	$\pi/4$	$I_x - Q_x - I_y - Q_y$	(1,-1,-1,-1)
$3\pi/4$	$\pi/4$	$-I_x - Q_x - I_y - Q_y$	(-1,-1,-1,-1)

After the 180° optical mixer and the balanced PD, we can get the real part I of the E'_x , which can be written as:

$$\frac{1}{\sqrt{2}} (I_x \cos \theta - Q_y \sin \theta - I_y \sin \phi - Q_y \cos \phi) \quad (9)$$

We can obtain arbitrary combination from $\pm I_x \pm I_y \pm Q_x \pm Q_y$ if appropriate phase shifts of θ and ϕ are set after normalization, which implies the binarized optical weights are applied to the I_x , I_y , Q_x , and Q_y , as shown in Table II.

IV. SIGNAL RECOVERY BASED ON OPTO-ELECTRONIC NEURAL NETWORK

A. Signal Recovery in Single Polarization System

In order to utilize the opto-electronic binarized neural network to recover the signal in the receiver, we first utilize the conventional coherent optical receiver to obtain the real part I and imaginary part Q of the signal. Then we design an ANN with three layers to recover the signal. The input layer and the output layer both have two neurons. The only hidden layer of the ANN has 16 neurons and is binarized including both the weights and activation, as shown in Fig. 5. The weights and activation of the output layer are real number and linear function, respectively. This ANN is trained using the transmitted and received signal. Then we extract the binarized weights of the first layer after the training is completed. All the inputs of the binarized hidden layer can be obtained, which are just the combination of I and Q with binarized weights.

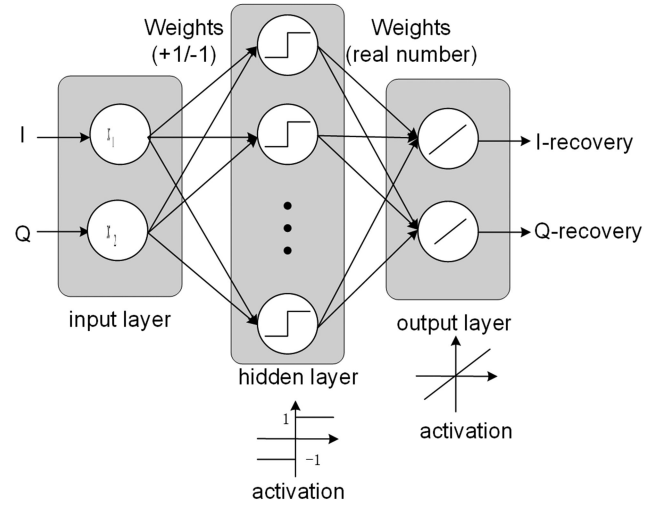


Fig. 5. Structure of ANN to recover the single polarization signal.

The binarized activations of the hidden layer can be regarded as the one-bit vertical resolution ADCs. Then we use the structure in Fig. 3 to map the combination of I and Q . As a result, an opto-electronic neural network is set up to recover the signal using one-bit vertical resolution ADCs, as shown in Fig. 6. Fig. 6 is the 50-Gb/s coherent optical communication system using binarized coherent optical receiver. At the transmitter, a 50-Gb/s QPSK signal is modulated by the optical I/Q modulator. Then the signal is launched into a fiber link consisting of standard single mode fiber (SSMF). The dispersion coefficient, PMD coefficient, and fiber nonlinearity refractive index of SSMF are 16 ps/(nm.km), 0.1 ps/km^{1/2} and 2.6×10^{20} m²/W. Then amplified spontaneous emission (ASE) is added to set (optical signal to noise ratio) OSNR. At the receiver, the broadcast layer is constituted by the MZIs for performing arbitrary linear optical processors [50]–[52]. In this system, we set the phase shifters of the MZIs to zero and the coupling coefficients of the couplers to 1/2, which could duplicate the received optical signal to 16 copies. In the broadcast layer, MZI is simple and easy to control compared with separation system. Realizing switching using MZIs based on silicon can reduce delay and energy consumption compared with using separation devices. Note that the device variance, imperfect tunings, chirp loss and SNR degradation introduced by the broadcast layer are not considered in the simulation. Then the optical signals are sent to the structures of optical binarized weights respectively to realize the weight mapping. After that the one-bit vertical resolution ADCs are used to convert the analog signals to digital signals, which are equal to the binarized activations. The last layer is just same as the output layer in Fig. 5, which is based on DSP in the electronic domain. Therefore, the function of this opto-electronic neural network is equal to the ANN in Fig. 5. Because the ANN in Fig. 5 has been trained successfully to recover the received signal, this opto-electronic neural network can also recover the received signal, but with only one-bit ADCs. Moreover, the broadcast layer and the optical layer can be integrated based on silicon, which could improve the calculation speed and lower the power

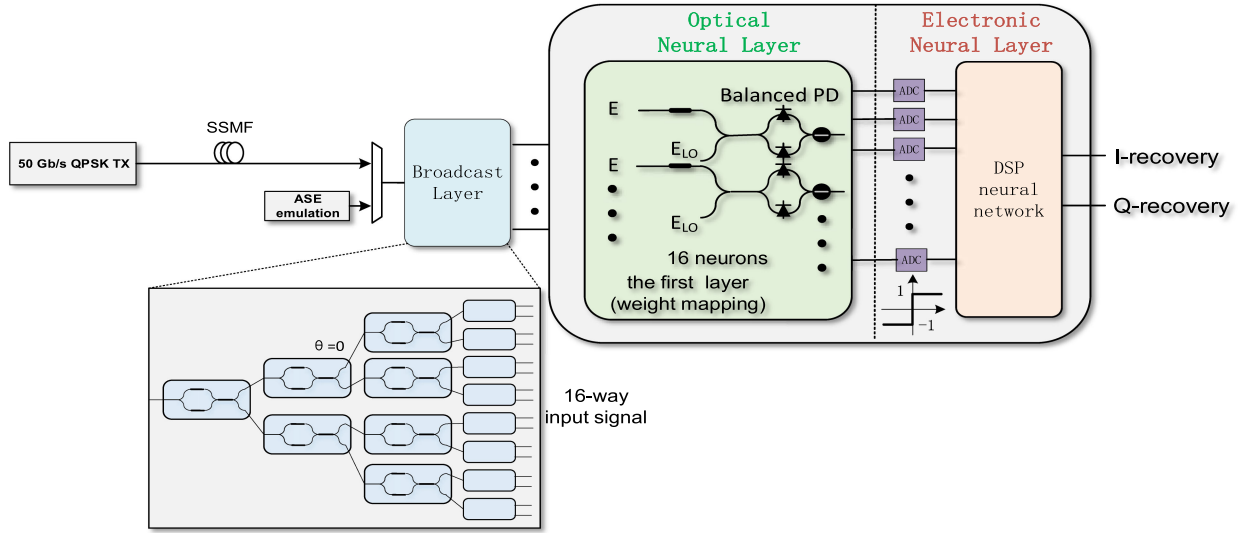


Fig. 6. 50-Gb/s CO-QPSK system with binarized coherent optical receiver. SSMF: standard single mode fiber.

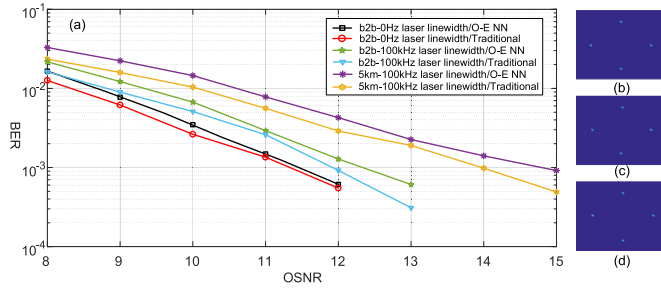


Fig. 7. (a) BER results of the 50-Gb/s CO-QPSK using the O-E NN based on 1-bit ADC and the traditional method based on 8-bit ADC after transmission of b2b-0 Hz laser linewidth, b2b-100 kHz laser linewidth, and 5 km-100 kHz laser linewidth, respectively; (b), (c), and (d) Recovered constellations after transmission of b2b-0 Hz laser linewidth, b2b-100kHz laser linewidth, and 5 km-100 kHz laser linewidth vs. OSNR 13 dB, 14 dB, 17 dB, respectively.

consumption of the total system. The neural network is used to recover the real part (I) and image part (Q) of the complex signal. After the neural network, we demodulate the complex signal to binary sequence. As last, the BER is obtained from the comparison between the received binary sequence and the transmitted binary sequence.

Fig. 7 is the simulation results of the SP system using the binarized coherent optical receiver. The number of the transmitted symbol is 16384. We use 9830 symbols as the training set and the remaining 6554 symbols as the testing set. Fig. 7(a) shows the BER results of the 50-Gb/s CO-QPSK using the opto-electronic neural network(O-E NN) based on 1-bit ADC and the traditional method based on 8-bit ADC after transmission of b2b-0 Hz laser linewidth, b2b-100 kHz laser linewidth, and 5 km-100 kHz laser linewidth, respectively. The BERs are pre-FEC (forward error correction) BER without FEC coding. Because the structure of the ANN in Fig. 5 does not consider the impairment in time correlation, the laser phase noise and the fiber impairments would degrade the system performance. Fig. 7 (b), (c), and (d) are

the recovered constellations of the b2b with 0-Hz laser linewidth versus (vs). OSNR of 13 dB, b2b with 100-kHz laser linewidth versus OSNR of 14 dB, and transmission over 5-km SSMF with 100-kHz laser linewidth vs. OSNR of 17 dB, respectively. A large amount of constellation points overlap at one point because of the binarized weights and activations. The ANN has done a hard decision to the constellation points. Therefore, the three constellations almost converge to four points but represent different BERs. Note that we do not into-account nonlinear effect in the simulation at present. If the nonlinear effect is considered, the neural network will be more complex and nonlinear activation functions should be utilized.

B. Signal Recovery in Polarization Multiplexing System

In the PDM optical communication system, there are two independent and orthogonal polarization signals. Similar with the single polarization system, in order to obtain the parameters of the opto-electronic neural network, conventional coherent optical receiver is utilized to obtain the real part I_x and I_y , and imaginary part Q_x and Q_y of the two polarization signals. The ANN with three layers is then applied to recover the signal, as shown in Fig. 8. The input layer and the output layer both have four neurons. The only hidden layer of the ANN also has 16 neurons and is binarized including both the weights and activation. The activation of the output layer is the linear function. The transmitted and received signal are utilized to train this ANN. After the training is completed, we extract the binarized weights of the first layer. All the inputs of the binarized hidden layer can be obtained, which are the combination of I_x , I_y , Q_x , and Q_y with the binarized weights.

Then the one-bit vertical resolution ADCs can be utilized as the binarized activations. The structure in Fig. 4 is used to construct the combination of I_x , I_y , Q_x , and Q_y . Consequently, the opto-electronic neural network for recovering the polarization multiplexing signals is set up with only the one-bit vertical

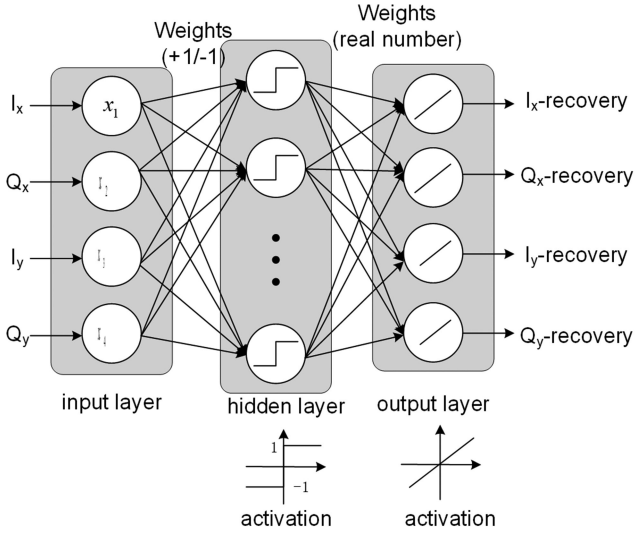


Fig. 8. Structure of ANN to recover the polarization multiplexing signal.

resolution ADCs, as shown in Fig. 9. Fig. 9 is the 100-Gb/s PDM-QPSK system using binarized coherent optical receiver. At the transmitter, a 100-Gbit/s PDM-QPSK signal contains two orthogonal polarization tributaries which have the same rate of 50-Gbit/s. The fiber link is also SSMF. The dispersion coefficient, PMD coefficient, and fiber nonlinearity refractive index are 16 ps/(nm.km), 0.1 ps/km^{1/2} and 2.6×10^{20} m²/W, respectively. Then ASE is added to set OSNR. At the receiver, a polarization beam splitter (PBS) is applied to split the optical signal into two orthogonal polarization states, *i.e.*, E_x and E_y . After that the two orthogonal signals are sent to the broadcast layer which is constituted by the MZIs [50]–[52]. In this system, we set the phase shifters of the MZIs to zero and the coupling coefficients of the couplers to 1 or 0. Then we could get E_x or E_y at any output port of the broadcast layer. Each pair of E_x and E_y is sent to the structure of Fig. 4 to map the binarized weights of the first layer of the ANN in Fig. 8. After that the one-bit vertical resolution ADCs are used to convert the analog signals to digital signals, which are equal to the binarized activations. The last layer is just same as the output layer of the ANN in Fig. 8, which is based on DSP in the electronic domain. Therefore, the function of this opto-electronic neural network is equal to the ANN in Fig. 8. Because the ANN in Fig. 8 has been trained successfully to recover the received PDM signals, this opto-electronic neural network can also recover the received PDM signals, and with only one-bit ADCs. Similar with the SP system, constructing the broadcast layer and optical layer using the silicon-based integrated analog optical signal processing could also increase the calculation speed and reduce the power consumption of the total system.

Fig. 10 is the simulation results of the polarization multiplexing system using the opto-electronic neural network. Fig. 10(a) shows the BER results of the 100-Gb/s PDM-CO-QPSK using the O-E NN based on 1-bit ADC and the traditional method based on 8-bit ADC after transmission of b2b-0 Hz laser

linewidth, b2b-100 kHz laser linewidth, and 5 km-100 kHz laser linewidth, respectively. The BERs are also pre-FEC BER without FEC coding. The laser phase noise and the fiber impairments also degrade the system performance because of the neglect of the crosstalk between symbols on time. Moreover, the binarized neural network needs more neurons and larger scale to reach the same performance compared with conventional neural network, the number of the first layer neuron in our neural network is not large enough to compensate the polarization effects. Fig. 10 (b), (c), and (d) are the recovered constellations of b2b with 0-Hz laser linewidth, b2b with 100-kHz laser linewidth, and transmission over 5-km SSMF with 100-kHz laser linewidth vs. OSNR of 20 dB, respectively. A large amount of constellation points also overlap at one point because of the binarized weights and activations. The nonlinear effect is also not taken into account in this simulation.

It should be noticed that the binarized weights and too few input eigenvalues of the first layer in the opto-electronic neural network would lead to a large number of wrong decisions for higher modulation formats. The proposed structure in this paper could not recover 16QAM and higher modulation formats at present. However, increasing the number of input eigenvalues or diversifying the weights of the first layer could solve this problem.

C. Speed Boost and Power Drop

In the conventional coherent optical receiver, 8-bit ADCs are utilized to convert analog signals to digital signals. Only DSP in the electronic domain is applied to recover the signal. The structure of DSP can be electronic neural network. In binarized coherent optical receiver, we put the first layer of the electronic neural network in the optical domain. The high-detection-rate, high-sensitivity photon detectors enable the optical neural network to be higher-speed and more energy-efficient compared with the electronic neural network. In principle, optical neural network can be at least two orders of magnitude faster than electronic neural networks because of the high speed optical devices [37]. Besides, in this structure, the average power consumption of maintaining one phase modulator is about 10 mW [37]. Especially, if the phases are set with nonvolatile phase-change materials [53], no power is needed to maintain, which can further reduce the power consumption of the binarized coherent optical receiver.

Compared with the conventional coherent optical receiver, another big advantage of the binarized coherent receiver is the reduction of the ADC resolution. In the single polarization conventional coherent optical receiver, as shown in Fig. 11, two 8-bit ADCs are applied while in our single polarization binarized coherent receiver, sixteen 1-bit ADCs are applied. High-speed especially beyond 1 GSample/s and high-resolution ADCs are very costly and power-hungry [54], [55]. In general, there are $2^n - 1$ comparator in a n -bit ADC. So the power consumption and cost increase exponentially with the resolution [54]. The power consumption of commercial ADCs always reaches level of Watts [55]. Therefore, reducing the resolution of ADCs is the

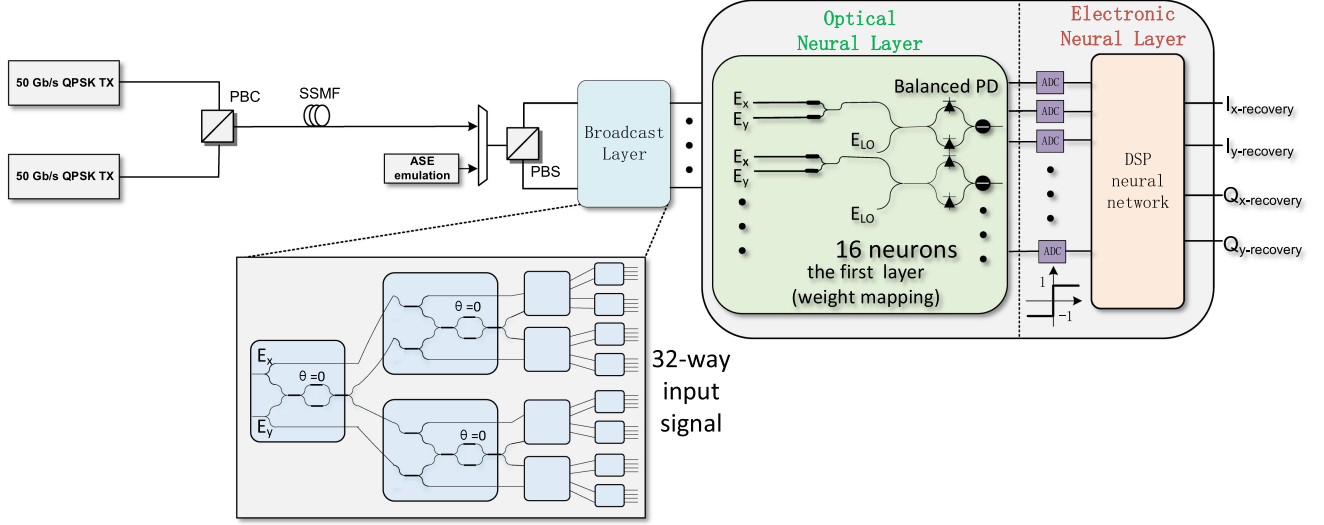


Fig. 9. 100-Gb/s PDM-CO-QPSK system with binarized coherent optical receiver. PBC: polarization beam combiner; PBS: polarization beam splitter; SSMF: standard single mode fiber.

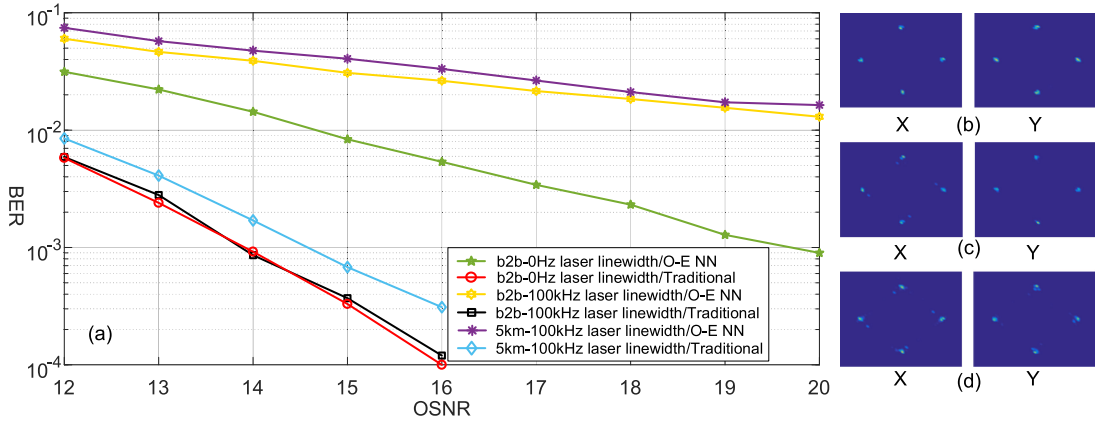


Fig. 10. (a) BER results of the 100-Gb/s PDM-CO-QPSK using the O-E NN based on 1-bit ADC and the traditional method based on 8-bit ADC after transmission of b2b-0 Hz laser linewidth, b2b-100 kHz laser linewidth, and 5 km-100 kHz laser linewidth, respectively; (b), (c), and (d) Recovered constellations after transmission of b2b-0 Hz laser linewidth, b2b-100kHz laser linewidth, and 5 km-100 kHz laser linewidth vs. OSNR 20 dB, respectively.

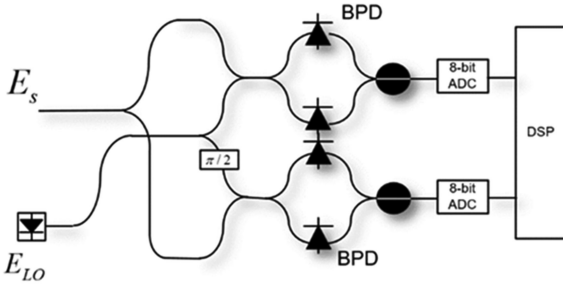


Fig. 11. Conventional coherent optical receiver.

V. CONCLUSION

In this paper, we have proposed a novel binarized coherent optical receiver based on opto-electronic neural network, which is applicable to both SP system and PDM system. Firstly, an ANN with binarized weights and activations in the first layer is designed and trained to recover the signal after conventional coherent detection. Then two special structures are designed to map the binarized weights in the optical domain for SP and PDM system respectively. There are three layers, *i.e.*, broadcast layer, optical neural layer, and electronic neural layer in the binarized coherent receiver. The received optical signal is firstly sent to the broadcast layer that composed of MZIs to duplicate and select the input optical signal to the opto-electronic neural network. Then the specially designed structure is utilized to construct the first layer of the opto-electronic neural network, which can be integrated together with the broadcast layer. The activations of

most effective approach to relieve the pressure of power consumption. The binarized coherent optical receiver only utilize 1-bit ADCs, which shows a big advantage in power consumption and cost.

the first layer are the one-bit vertical resolution ADCs, which convert the analog signals to binarized digital signals. At last, the binarized digital signals flow into the following electronic neural layers with conventional weights and activations to recover the signal. We have demonstrated this binarized coherent optical receiver in simulation of 50-Gb/s SP-QPSK system and 100-Gb/s PDM-QPSK system. The simulation results show that the binarized coherent optical receiver with low cost ADCs of one-bit vertical resolution could recover the signal with complex modulation format successfully. Moreover, constructing the first layer of the ANN using the silicon-based integrated analog optical signal processing could also increase the calculation speed and reduce the power consumption of the total system.

REFERENCES

- [1] T. Li, "Upgrading lightwave transmission capacity with wavelength-multiplexing and high-speed technologies," in *Proc. IEEE/LEOS 1995 Dig. LEOS Summer Top. Meetings*, 1995, p. 25.
- [2] L. W. Luo *et al.*, "WDM-compatible mode-division multiplexing on a silicon chip," *Nature Commun.*, vol. 5, Jan. 2014, Art. no. 3069.
- [3] A. Ramaswamy *et al.*, "A WDM 4×28 Gbps integrated silicon photonic transmitter driven by 32nm CMOS driver ICs," in *Proc. Opt. Fiber Commun. Conf.*, Los Angeles, CA, USA, 2015, Paper Th5B.5.
- [4] J. Tang, "A comparison study of the shannon channel capacity of various nonlinear optical fibers," *J. Lightw. Technol.*, vol. 24, no. 5, pp. 2070–2075, May 2006.
- [5] H. Hu *et al.*, "Fiber nonlinearity compensation by repeated phase conjugation in 2.048-Tbit/s WDM transmission of PDM 16-QAM channels," in *Proc. Opt. Fiber Commun. Conf.*, Anaheim, CA, USA, Mar. 2016, Paper Th4F.3.
- [6] D. M. Marom and M. Blau, "Switching solutions for WDM-SDM optical networks," *IEEE Commun. Mag.*, vol. 53, no. 2, pp. 60–68, Feb. 2015.
- [7] K. Kikuchi and S. Tsukamoto, "Evaluation of sensitivity of the digital coherent receiver," *J. Lightw. Technol.*, vol. 26, no. 13, pp. 1817–1822, Jul. 2008.
- [8] R.-J. Essiambre, G. Kramer, P. J. Winzer, G. J. Foschini, and B. Goebel, "Capacity limits of optical fiber networks," *J. Lightw. Technol.*, vol. 28, no. 4, pp. 662–701, Feb. 2010.
- [9] W. Shieh and C. Athaudage, "Coherent optical orthogonal frequency division multiplexing," *Electron. Lett.*, vol. 42, no. 10, pp. 587–589, May 2006.
- [10] S. J. Savory, "Digital filters for coherent optical receivers," *Opt. Express*, vol. 16, no. 2, pp. 804–817, 2008.
- [11] E. Ip, A. P. T. Lau, D. J. Barros, and J. M. Kahn, "Coherent detection in optical fiber systems," *Opt. Express*, vol. 16, no. 2, pp. 753–791, Jan. 2008.
- [12] P. Marin-Palomo *et al.*, "Microresonator-based solitons for massively parallel coherent optical communications," *Nature*, vol. 546, no. 7657, pp. 274–279, 2017.
- [13] A. Mecozzi, C. Antonelli, and M. Shtaif, "Kramers–Kronig coherent receiver," *Optica*, vol. 3, no. 11, pp. 1220–1227, 2016.
- [14] M. Qiu *et al.*, "Digital subcarrier multiplexing for fiber nonlinearity mitigation in coherent optical communication systems," *Opt. Express*, vol. 22, no. 55, pp. 18770–18777, Jul. 2014.
- [15] J. Zhang, W. Chen, M. Gao, and G. Shen, "K-means-clustering-based fiber nonlinearity equalization techniques for 64-QAM coherent optical communication system," *Opt. Express*, vol. 25, no. 22, pp. 27570–27580, 2017.
- [16] J. Yu and X. Zhou, "Ultra-high-capacity DWDM transmission system for 100 G and beyond," *IEEE Commun. Mag.*, vol. 48, no. 3, pp. S56–S64, Mar. 2010.
- [17] E. Agrell *et al.*, "Roadmap of optical communications," *J. Opt.*, vol. 18, 2016, Art. no. 063002.
- [18] J. Yu *et al.*, "400 Gb/s (4 100 Gb/s) orthogonal PDM-RZ-QPSK DWDM signal transmission over 1040 km SMF-28," *Opt. Express*, vol. 17, no. 20, pp. 17928–17933, 2009.
- [19] T. Wuth, M. W. Chbat, and V. F. Kamalov, "Multi-rate (100G/40G/10G) transport over deployed optical networks," in *Proc. Conf. Opt. Fiber Commun.*, San Diego, CA, USA, 2008, Paper NtuB3.
- [20] C. R. S. Fludger *et al.*, "Coherent equalization and POLMUX-RZ-DQPSK for robust 100-GE transmission," *J. Lightw. Technol.*, vol. 26, no. 1, pp. 64–72, Jan. 2008.
- [21] H. Sun *et al.*, "Modulation formats for 100 Gb/s coherent optical systems," in *Proc. Opt. Fiber Commun.*, San Diego, CA, USA, 2009, Paper OTuN1.
- [22] M. P. Yankov *et al.*, "Constellation shaping for WDM systems using 256QAM/1024QAM with probabilistic optimization," *J. Lightw. Technol.*, vol. 34, no. 22, pp. 5146–5156, Nov. 2016.
- [23] S. Beppu, K. Kasai, M. Yoshida, and M. Nakazawa, "2048 QAM (66 Gbit/s) single-carrier coherent optical transmission over 150 km with a potential SE of 15.3 bit/s/Hz," *Opt. Express*, vol. 23, no. 4, pp. 4960–4969, Feb. 2015.
- [24] D. Qian, E. Ip, M.-F. Huang, M.-J. Li, and T. Wang, "698.5-Gb/s PDM-2048QAM transmission over 3 km multicore fiber," in *Proc. Eur. Conf. Opt. Commun.*, London, U.K., Sep. 2013, Paper Th.1.C.5.
- [25] P. J. Winzer, D. T. Neilson, and A. R. Chraplyvy, "Fiber-optic transmission and networking: The previous 20 and the next 20 years," *Opt. Express*, vol. 26, pp. 24190–24239, 2018.
- [26] J. Leuthold, C. Koos, and W. Freude, "Nonlinear silicon photonics," *Nature Photon.*, vol. 4, pp. 535–544, 2010.
- [27] C. Koos, L. Jacome, C. Poulton, J. Leuthold, and W. Freude, "Nonlinear silicon-on-insulator waveguides for all-optical processing," *Opt. Express*, vol. 15, pp. 5976–5990, 2007.
- [28] D. A. B. Miller, "Are optical transistors the logical next step?," *Nature Photon.*, vol. 4, no. 1, pp. 3–5, 2010.
- [29] A. E. Willner, S. Khaleghi, M. R. Chitgarha, and O. F. Yilmaz, "All-optical signal processing," *J. Lightw. Technol.*, vol. 32, no. 4, pp. 660–680, Feb. 2014.
- [30] B. J. Eggleston *et al.*, "Photonic chip based ultrafast optical processing based on high nonlinearity dispersion engineered chalcogenide waveguides," *Laser Photon. Rev.*, vol. 6, pp. 97–114, 2012.
- [31] D. Liang and J. E. Bowers, "Recent progress in lasers on Silicon," *Nature Photon.*, vol. 4, no. 8, pp. 511–517, 2010.
- [32] L. Chen *et al.*, "Electronic and photonic integrated circuits for fast data center optical circuit switches," *IEEE Commun. Mag.*, vol. 51, no. 9, pp. 53–59, Sep. 2013.
- [33] T. Komljenovic *et al.*, "Heterogeneous silicon photonic integrated circuits," *J. Lightw. Technol.*, vol. 34, no. 1, pp. 20–35, Jan. 2016.
- [34] M. J. R. Heck *et al.*, "Hybrid silicon photonic integrated circuit technology," *IEEE J. Sel. Topics Quantum Electron.*, vol. 19, no. 4, Jul./Aug. 2013, Art. no. 6100117.
- [35] M. H. Khan *et al.*, "Ultrabroad-bandwidth arbitrary radiofrequency waveform generation with a silicon photonic chip-based spectral shaper," *Nature Photon.*, vol. 4, pp. 117–122, 2010.
- [36] A. N. Tait *et al.*, "Neuromorphic silicon photonics," 2016, *arXiv:1611.02272*.
- [37] Y. Shen *et al.*, "Deep learning with coherent nanophotonic circuits," *Nature Photon.*, vol. 11, pp. 441–446, 2017.
- [38] T. W. Hughes, M. Minkov, Y. Shi, and S. Fan, "Training of photonic neural networks through *in situ* backpropagation and gradient measurement," *Optica*, vol. 5, no. 7, pp. 864–871, 2018.
- [39] X. Lin *et al.*, "All-optical machine learning using diffractive deep neural networks," *Science*, vol. 361, no. 6406, pp. 1004–1008, 2018.
- [40] Y. LeCun, Y. Bengio, and G. Hinton, "Deep learning," *Nature*, vol. 521, pp. 436–444, 2015.
- [41] G. Hinton *et al.*, "Deep neural networks for acoustic modeling in speech recognition," *IEEE Signal Process. Mag.*, vol. 29, no. 6, pp. 82–97, Nov. 2012.
- [42] A. J. M. Timmermans, and A. A. Hulzebosch, "Computer vision system for on-line sorting of pot plants using an artificial neural network classifier," *Comput. Electron. Agriculture*, vol. 15, no. 1, pp. 41–55, 1996.
- [43] J. V. Tu, "Advantages and disadvantages of using artificial neural networks versus logistic regression for predicting medical outcomes," *J. Clin. Epidemiology*, vol. 49, no. 11, pp. 1225–1231, 1996.
- [44] C. Yan *et al.*, "Supervised hash coding with deep neural network for environment perception of intelligent vehicles," *IEEE Trans. Intell. Transp. Syst.*, vol. 19, no. 1, pp. 284–295, Jan. 2018.
- [45] M. Courbariaux and Y. Bengio, "BinaryNet: Training deep neural networks with weights and activations constrained to +1 or -1," 2016, *arXiv:1602.02830*.
- [46] T. J. O'Shea and J. Hoydis, "An introduction to deep learning for the physical layer," *IEEE Trans. Cogn. Commun. Netw.*, vol. 3, no. 4, pp. 563–575, Dec. 2017.
- [47] J. Estaran *et al.*, "Artificial neural networks for linear and non-linear impairment mitigation in high-baudrate IM/DD systems," in *Proc. Eur. Conf. Opt. Commun.*, 2016, Paper M.2.B.2.

- [48] M. A. Jarajreh *et al.*, “Artificial neural network nonlinear equalizer for coherent optical OFDM,” *IEEE Photon. Technol. Lett.*, vol. 27, no. 4, pp. 387–390, Feb. 2015.
- [49] A. Argyris, J. Bueno, and I. Fischer, “Photonic machine learning implementation for signal recovery in optical communications,” *Sci. Rep.*, vol. 8, no. 1, 2018, Art. no. 8487.
- [50] A. Ribeiro, A. Ruocco, L. Vanacker, and W. Bogaerts, “Demonstration of a 4×4 -port universal linear circuit,” *Optica*, vol. 3, no. 12, pp. 1348–1357, 2016.
- [51] D. A. B. Miller, “Self-configuring universal linear optical component,” *Photon. Res.*, vol. 1, pp. 1–15, 2013.
- [52] D. A. B. Miller, “Perfect optics with imperfect components,” *Optica*, vol. 2, pp. 747–750, 2015.
- [53] Q. Wang *et al.*, “Optically reconfigurable metasurfaces and photonic devices based on phase change materials,” *Nature Photon.*, vol. 10, no. 1, pp. 60–65, 2016.
- [54] R. Walden, “Analog-to-digital converter survey and analysis,” *IEEE J. Sel. Areas Commun.*, vol. 17, no. 4, pp. 539–550, Apr. 1999.
- [55] B. Le, T. Rondeau, J. Reed, and C. Bostian, “Analog-to-digital converters,” *IEEE Signal Process. Mag.*, vol. 22, no. 6, pp. 69–77, Nov. 2005.

Zhenming Yu received the B.Eng. degree in electronic science and technology and the M.Eng. degree in optical engineering from the University of Electronic Science and Technology of China (UESTC), Chengdu, China, in 2011 and 2014, respectively, and the Ph.D. degree in electronic science and technology from Tsinghua University, Beijing, China, in 2018. He is currently with the State Key Laboratory of Information Photonics and Optical Communications, Beijing University of Posts and Telecommunications, Beijing, China. His current research interests are photonics neural networks, and optical and digital signal processing for coherent and direct-detection optical communication.

Xu Zhao received the B.E. degree in electronic engineering from Tsinghua University, Beijing, China, in 2016. He is currently working toward the M.Eng. degree in electronic science and technology at Tsinghua University, Beijing, China. His current research interests are silicon-based photonics and photonics neural network.

Sigang Yang received the Ph.D. degree from Tsinghua University, Beijing, China, in 2008. He is involved in research of the theory and technology of photonic crystal fiber and nonlinear optics. He is the author or coauthor of more than 50 journal and conference papers. His research activities have covered a board range of fiber optic parametric amplifier and optical parametric oscillator optical modulation, computational electromagnetics in fiber, and all-optical wavelength conversion long-haul transmission links and optical access networks. His current research interests include silicon-based frequency comb and terahertz.

Hongwei Chen (M’07) was born in Inner Mongolia, China, in 1979. He received the B.E. and Ph.D. degrees in electronic engineering from Tsinghua University, Beijing, China, in 2001 and 2006, respectively. He is currently with the Faculty of the Department of Electronic Engineering, Tsinghua University. His current research interests include radio-over-fiber techniques, high-speed optical communications, and optical packet switching networks. Dr. Chen received the Best Student Paper Award of Asia-Pacific Optical Communications (APOC) 2004 and was a Subcommittee Member of APOC 2005, 2007, 2008, and Pacific Rim Conference on Lasers and Electro-Optics (CLEO-PR) 2007.

Minghua Chen (M’04) received the Ph.D. degree in electronics engineering from Southeast University, Nanjing, China, in 1998. From 1998 to 2000, he was a Postdoctoral Researcher with Tsinghua University, where he is currently the Vice Director of the Information Optoelectronics Research Center within the Department of Electronics Engineering. He has supervised and collaborated on several projects supported by the Chinese National Science Funds and High-Tech (863) Projects. His current research interests include optical networking and its key technologies, including dynamical wavelength routing, optical label switching, optical packet switching, and their key optical components.